International Symposium
On Turbulence and Shear Flow
Phenomena (TSFP-8)
August 28 - 30, 2013 Poitiers, France

HIGH RESOLUTION VELOCITY PROFILE MEASUREMENTS IN TURBULENT BOUNDARY LAYERS

Christian J. Kähler, Sven Scharnowski, Christian Cierpka
Institute of Fluidmechanics and Aerodynamics
Bundeswehr University Munich
85577 Neubiberg, Germany
christian.kaehler@unibw.de

ABSTRACT

Particle Image Velocimetry (PIV) is an established technique for the measurement of instantaneous or time resolved flow fields in two and three dimensions. As no other technique is able to determine quantitatively unsteady flow field information, PIV has evolved to the leading measurement technique in fluid mechanics over the last decade. However, for the measurement of mean velocity profiles and turbulent velocity fluctuations hot-wire probes and laser Doppler anemometer are still the most established techniques, because they are simpler to use and often more precise than PIV. In this paper it is shown how the lack of accuracy can be compensated by using more advanced PIV evaluation techniques. This is very beneficial because PIV allows to measure without any traversing the instantaneous and average flow information at thousands of points simultaneously. In this case measurement errors caused by long time variations of the wind tunnel speed, viscosity, temperature and humidity effects or errors associate with the mechanical traversing the probe to thousands of points or effects due to probe vibrations cannot take place. In order to enhance the measurement accuracy of the PIV technique the authors have developed sophisticated image analysis techniques in the last years (Scharnowski *et al.*, 2012; Kähler *et al.*, 2012*a*,*b*; Cierpka *et al.*, 2013*b*,*a*). In this contribution these techniques are used to evaluate the measurements of a turbulent boundary layer flow along a flat plate in the 22 m long and 2 by 2 square-meter wide test section of the Atmospheric Wind tunnel at UniBw Munich. Beside the mean velocity fields also the capabilities in estimating turbulent quantities such as the Reynolds stresses and the probability density function of the velocity fluctuations is outlined. There is still some work which needs to be done, but the results already indicate the potential of the developed evaluation techniques in estimating averaged flow quantities.

MOTIVATION

Digital particle image velocimetry (DPIV) has become one of the most widespread techniques for the investigation of turbulent flows in the last decades because it allows for the instantaneous measurement of the flow field without disturbing the flow or fluid properties. Moreover, this technique presents the advantage that spatial flow features can be resolved and gradient-based quantities such as the vorticity can be calculated. In addition, correlation and spectral methods can be applied to analyze the velocity fields. Frequently, the technique is also applied to efficiently measure average quantities such as mean velocity or Reynolds stress distributions because these are still the most relevant variables for the validation of numerical flow simulations and the verification or disproof of theories or models in fluid mechanics. Unfortunately, the accuracy of the measurement technique is often not high enough to determine the averaged quantities with the desired precision. The main reasons are 1. bias errors caused by the finite size of the correlation volume in case of flow gradients (Keane & Adrian, 1992; Westerweel, 2008; Scarano, 2001; Kähler *et al.*, 2012*a*), 2. large random errors in case of small particle image shifts (Stanislas *et al.*, 2008; Hain & Kähler, 2007) and 3. position errors due to the finite thickness of the light sheet and vibrations of the model or measurement equipment (Westerweel *et al.*, 2013; Cierpka *et al.*, 2013*b*).

In the last year, new concepts for the evaluation of PIV recordings were developed at the Bundeswehr University Munich with the aim of enhancing the spatial resolution by more than two orders of magnitude (Kähler *et al.*, 2012*a*,*b*; Scharnowski *et al.*, 2012). This allows to estimate high resolution flow fields without bias errors, which are typical for conventional cross-correlation PIV analysis but also for other measurement techniques such as hot-wire and LDV. Furthermore, multiframe evaluation techniques were developed to minimize the random errors (Hain & Kähler, 2007; Cierpka *et al.*, 2013*a*) and finally, methods to compensate vibrations of the model and measurement equipment have been developed and approaches to calibrated errors due to the finite thickness of the light sheet (Cierpka *et al.*, 2013*b*).

In this contribution the technical developments were used to determine the flow characteristics of a turbulent boundary layer at large Reynolds number. The measurement was performed in the Atmospheric Windtunnel at the Institute of Fluid Mechanics and Aerodynamics of the Bundeswehr University Munich. The facility has a 22 m long test section with a 2 m by 2 m cross section. Measurements were performed at a free stream velocity of 11 m/s. The combination of different optical setups with different magnifications allowed for the simultaneous measurement of the outer variables such as boundary layer thickness and free stream velocity using single-pixel ensemble-correlation (Kähler *et al.*, 2006) and the near-wall flow profile using PTV (Cierpka *et al.*, 2013*b*). A schematic of the wind tunnel and an overview of the different fields of view (FOV) applied, are shown in Fig. 1. For the image recording, two sCMOS cameras (with a working distance of 1 m) were

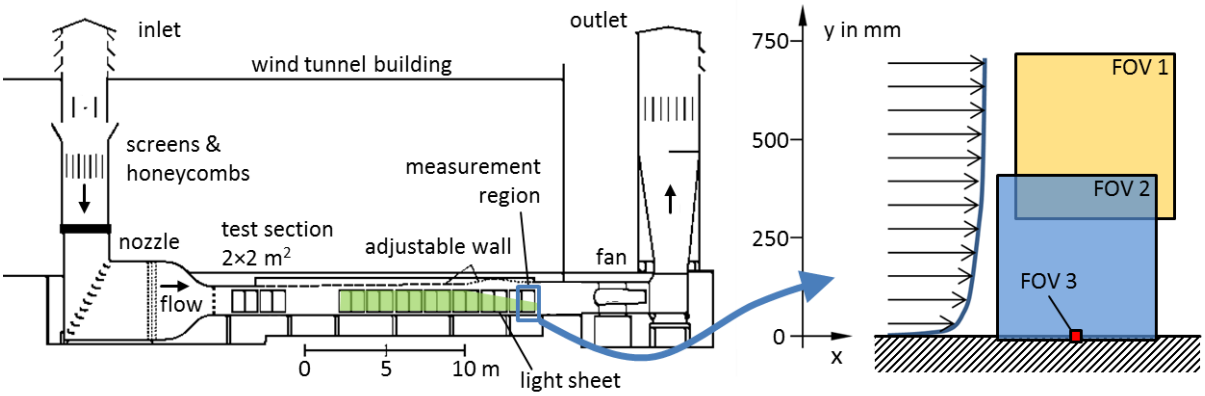

Figure 1. Large scale Eiffel type wind tunnel at the Bundeswehr University in Munich (left). Different fields of view according to Tab. 1 (right).

used. For the large field of view experiments (FOV 1 and 2) a Zeiss Distagon T* 1.4/35 mm objective lens was mounted to the camera. The high magnification experiments (FOV 3) were performed using a long-distance microscope system (K2 by Infinity, Kähler *et al.* (2006)). For FOV 1 and 2 the particle image density was adjusted to 0.035 particles per pixel for a reliable and efficient velocity measurement with correlation-based evaluation methods. For FOV 3 this concentration results in a particle image density of $1.9 \cdot 10^{-4}$ which is well suited for a reliable tracking of individual particle images. Thus, the large and small FOV can be observed simultaneously.

The wall-normal extension of the FOV, the optical magnification and the resulting scale as well as the digital particle image diameter and particle image density are summarized in Tab. 1. To illuminate the one micron DEHS particles, which were injected in the inlet before the screens of the wind tunnel, the beam of the Spectra Physics Quanta-Ray PIV 400 Nd:YAG double-pulse laser was shaped into a light sheet by using a set of spherical and cylindrical lenses outside of the wind tunnel. To illuminate the measurement region a mirror was installed close to the fan of the wind tunnel. This mirror reflects the light sheet in upstream direction such that the light sheet is only grazing the bottom wall. This allows to prevent strong scattering, which is disadvantageous for the detection of particle images close to walls (Kähler *et al.*, 2006). The wind tunnel wall was polished at the measurement location to further decreases any diffuse scattering by the wall. This approach is required for making near wall measurements possible, but also for the application of the developed method to compensate the perspective error outlined in the following section.

MEAN VELOCITY PROFILE

Figure 2 shows exemplary the averaged turbulent boundary layer velocity profile. The different color of the measurement points indicate the different evaluation techniques applied for the analysis of the data set. The red graph, which was evaluated with single-pixel ensemble-correlation, covers the macroscopic flow features from the buffer layer to the outer edge of the boundary layer. Only the buffer layer and the viscous sub-layer cannot be resolved properly using this evaluation technique with the specific optical settings as the spatial resolution is limited to 350 μm in wall-normal direction (Kähler *et al.*, 2012*a*). Therefore, PTV evaluation techniques are applied to estimate the wall-shear-stress directly from the velocity profile in the viscous sub-layer (Kähler *et al.*, 2012*b*). However, the enhanced resolution also requires a compensation of all microscopic vibrations of the facility and measurement equipment by using digital image analysis techniques. This is obvious because vibrations of the wind tunnel with an amplitude of 4 microns would already lower the spatial resolution by a factor of two. The black graph in Fig. 2 shows the improvement in spacial resolution by using PTV algorithms. However, due to the high spatial resolution an additional systematic measurement error can be observed, see drop of measurement point at $y < 80$ microns or $y^+ < 2$ in Fig 2. This error is caused by the finite thickness of the light sheet, as illustrated in Fig. 3. In order to avoid optical distortions by a half coverage of the objective lens, the objective lens is typically placed right above the wall if the observation distance is sufficiently large. This set-up is shown in the upper part of the figure. The measured particle image with its diffraction rings can be seen on the right part of the same figure. Due to the finite width of the light sheet a perspective error is introduced which vanishes along the optical axis. This so called parallax error is a common problem for long-focal length systems, e.g., in astronomy (van de Kamp, 1963). The further away from the optical axis a particle image is and thus the closer to the wall, the larger is the perspective error. Particle images that have the same

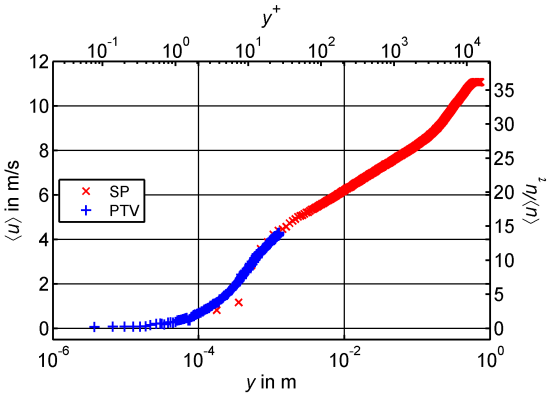

Figure 2. Mean velocity profile.

Table 1. Parameter of the setup.

FOV	wall-normal range in mm	magnification	scaling in px/μm	particle image diameter D_I in px	particle image density in ppp
1	300 – 740	0.04	173	2-3	0.035
2	-11 – 438	0.04	177	2-3	0.035
3	-1.8 – 9.1	1.52	4.3	10-25	$1.9{\cdot}10^{-4}$

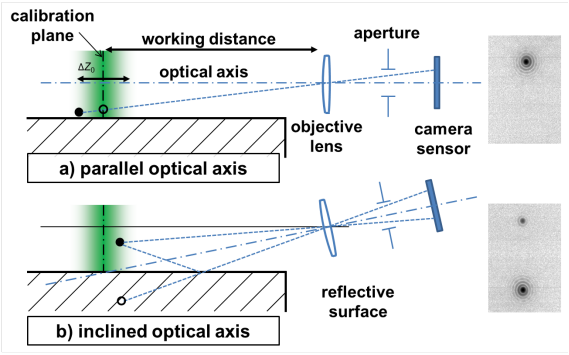

Figure 3. Parallax correction by using mirrored particle images.

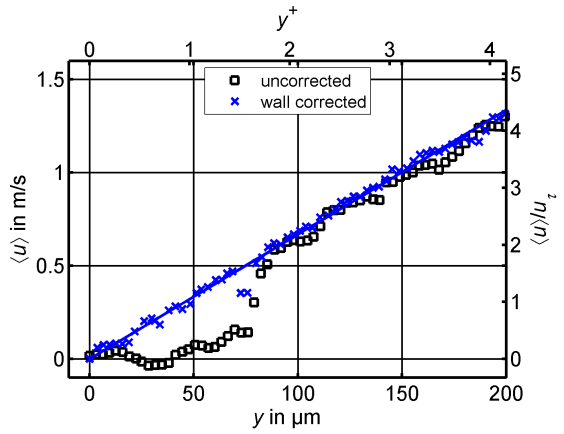

Figure 4. Close up of the near-wall region.

y-position in the image space can have different positions above the wall depending on their axial position z within the light sheet. In order to minimize the perspective error close to the wall the optical axis can be tilted to image the surface of the wall at the position of the optical axis. This setup is shown in the lower part of the figure. By using a reflective surface (polished metal or glass) a mirror image can be seen. By taking the information from the actual particle image and its mirrored counterpart, the wall-normal distance can be corrected for the perspective errors. For the details of the method, the interested reader is referred to Cierpka *et al.* (2013*b*).

By using a special evaluation strategy, which compensates this effect completely, also the viscous sub-layer is nicely resolved with 50 independent data points, as indicated in the blue graph in Fig. 3. The wall-shear-stress τ_w and the shear velocity u_τ were estimated by a direct fit of the data points for $y^+ < 4$. By using the uncorrected PTV results, the following values could be estimated: $\tau_w = 0.111 \pm 0.0045$ in N/m^2 and $u_\tau = 0.308 \pm 0.0038$ m/s. For the wall-position corrected PTV results the wall-shear-stress was estimated to be $\tau_w = 0.110 \pm 0.0043$ in N/m^2 and $u_\tau = 0.307 \pm 0.0037$ m/s. Thus, the direct estimation of u_τ works very precise by using PTV evaluation techniques with shift correction and perspective error compensation. The precision of the data is also very good in comparison with the data published by other authors. However, by using multi-frame recording and evaluation technique, the precision can be further enhanced, as discussed in Cierpka *et al.* (2013*b*). Table 2 shows the measurement parameters for the macroscopic and for the microscopic approach. Table 3 summarizes the main results obtained for the data.

Table 2. Measurement parameters.

	Macroscopic	Microscopic
FOV in mm	$-11 < y < 740$	$-1.8 < y < 9.1$
Magnification	0.04	1.52
Scale	175 μm/px	4.3 μm/px
D	2 – 3 px	10 – 25 px

Table 3. Evaluation results.

Quantity	Value
u_∞	11.06 ± 0.02 m/s
δ_{99}	535 ± 3 mm
Re_δ	$0.4 \cdot 10^6$
u_τ	0.307 ± 0.004
τ_w	0.110 ± 0.004

PROBABILITY DENSITY FUNCTION

In order to obtain more information about the turbulent boundary layer flow at large Reynolds number, the probability density function of the stream wise velocity fluctuations was estimated for the near-wall region where the distribution is not Gaussian. Figure 5 shows that the PTV technique applied for the evaluation of the data is well suited to resolve the distribution. The green graph are estimated with the wall-correction technique and the red one without. At $y^+ = 1$ a significant difference can be seen between the results but for $y^+ = 2$ and larger the difference become less and less pronounced. This shows the need for the special calibration method for reliable near wall turbulence measurements. The expected non-Gaussian distribution is clearly visible for the lower wall locations, and at $y^+ = 20$ the distribution appears almost symmetric. The analysis shows that even higher order moments can be reliable measured by using the developed evaluation technique. To get fully converged values, more data sets must be evaluated and by using multi-frame evaluation techniques (Cierpka *et al.*, 2013*a*) the precision can be further increased by an order of magnitude. However, the potential of the advanced recording and evaluation technique is already obvious.

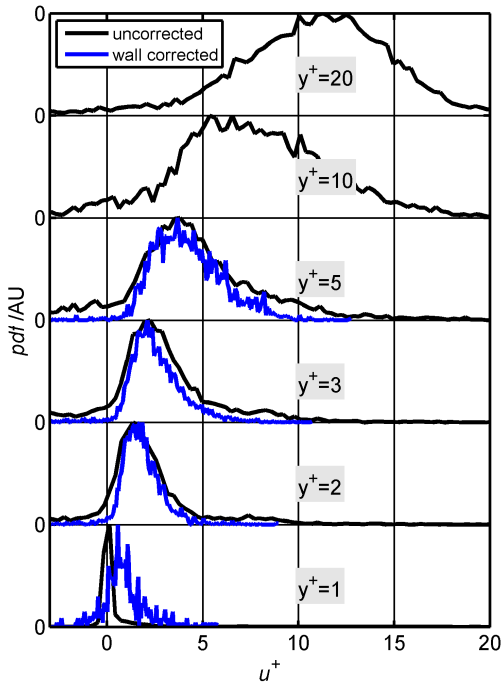

Figure 5. Probability density function of the wall-parallel velocity component.

REYNOLDS STRESS

Finally, profiles of the RMS value of the stream-wise velocity fluctuation are shown in Fig. 6. The values in the outer region (red) were computed from the shape of the correlation function by using single-pixel ensemble-correlation, as discussed in Scharnowski *et al.* (2012). The stresses in the buffer layer and in the viscous region were

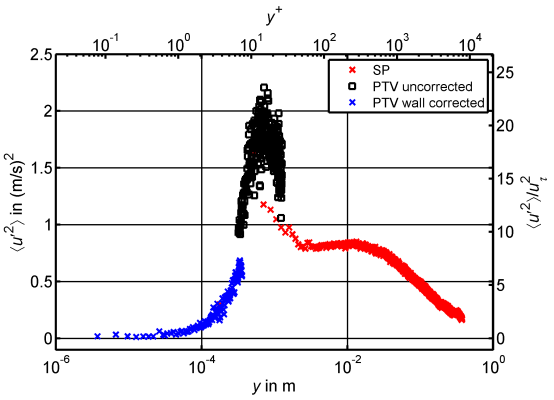

Figure 6. Streamwise turbulence intensity.

estimated by using PTV, as outlined before. The wall-normal location of the two maxima in Fig. 6 at $y^+ \approx 20$ and $y^+ \approx 300$ corresponds to values presented in Fernholz & Finley (1996) or Marusic *et al.* (2010). The stress values for the inner peak is significantly larger. However, as the number of samples is not sufficiently high further measurements are required to estimate the exact values with this technique. Nevertheless, the potential of the technique in estimating turbulence quantities is demonstrated.

CONCLUSIONS

The analysis shows that the PIV ensemble correlation image analysis with up to single-pixel resolution is very well suited to resolve the velocity profile properly even for large field of view recordings. Also, the estimation of the boundary layer thickness can be performed reliably and the relative uncertainty was below 1% for the Reynolds numbers considered here. However, the large field of view recording limits the spatial resolution to 5 wall units. Therefore, the direct wall-shear-stress estimation requires a high magnification recording configuration and a PTV evaluation technique in order to avoid bias errors associated with the correlation analysis. By using PTV algorithms, the resolution is not limited by the particle image diameter, as in the case of the single-pixel ensemble-correlation approach.

For $Re = 0.4 \cdot 10^6$ a resolution of 0.1 wall units was achieved, leading to 50 independent data points in the viscous sub-layer. This allow to determine the wall-shear-stress directly by a fit function. Beside the mean velocity also the turbulent fluctuations and the probability density function of the velocity fluctuations could be measured with the techniques. Thus, by combining the strength of each evaluation method the reliable estimation of many relevant flow quantities is possible within a short measurement time and without traversing of the probe. In addition vibrations of the model or measurement equipment can be compensated completely by using digital image analysis methods, so that these bias errors do not affect the near wall PTV measurements at all. The results show that the high resolution gives access to quantities, which make a deeper analysis of the turbulent processes possible. Thus, PIV and PTV might become a standard even for profile measurements in the future, like hot wire probes or laser Doppler anemometer today.

ACKNOWLEDGMENTS

The financial support from the European Communitys Seventh Framework program (FP7/2007-2013) under grant agreement No. 265695 and from the German research foundation (DFG) under the individual grants program KA 1808/8 and the transregio program TRR40 is gratefully acknowledged.

REFERENCES

Cierpka, C., Lütke, B. & Kähler, C. J. 2013*a* Higher order multi-frame particle tracking velocimetry. *Exp Fluids* **54** (5), 1–12.

Cierpka, C., Scharnowski, S. & Kähler, C. J. 2013*b* Parallax correction for precise near-wall flow investigations using particle imaging. *Applied Optics* **52**, 2923–2931.

Fernholz, H. H. & Finley, P. J. 1996 The incompressible zero-pressure-gradient turbulent boundary layer: an assessment of the data. *Progress in Aerospace Sciences* **32** (4), 245–311.

Hain, R. & Kähler, C. J. 2007 Fundamentals of multiframe particle image velocimetry (PIV). *Exp Fluids* **42**, 575–587ll.

Kähler, C. J., Scharnowski, S. & Cierpka, C. 2012*a* On the resolution limit of digital particle image velocimetry. *Exp Fluids* **52**, 1629–1639.

Kähler, C. J., Scharnowski, S. & Cierpka, C. 2012*b* On the uncertainty of digital PIV and PTV near walls. *Exp Fluids* **52**, 1641–1656.

Kähler, C. J., Scholz, U. & Ortmanns, J. 2006 Wall-shear-stress and near-wall turbulence measurements up to single pixel resolution by means of long-distance micro-PIV. *Exp Fluids* **41**, 327–341.

van de Kamp, P. 1963 Problems of Long-Focus Photographic Astrometry. *Applied Optics* **2**, 9–15.

Keane, R. D. & Adrian, R. J. 1992 Theory of cross-correlation analysis of PIV images. *Applied Scientific Research* **49**, 191–215.

Marusic, I., McKeon, B. J., Monkewitz, P. A., Nagib, H. M., Smits, A. J. & Sreenivasan, K. R. 2010 Wall-bounded turbulent flows at high Reynolds numbers: Recent advances and key issues. *Phys Fluids* **22**, 065103.

Scarano, F. 2001 Iterative image deformation methods in PIV. *Meas Sci Tech* **13**, R1–R19.

Scharnowski, S., Hain, R. & Kähler, C. J. 2012 Reynolds stress estimation up to single-pixel resolution using PIV-measurements. *Exp Fluids* **52**, 985–1002.

Stanislas, M., Okamoto, K., Kähler, C. J., Westerweel, J. & Scarano, F. 2008 Main results of the third international PIV Challenge. *Exp Fluids* **45**, 27–71.

Westerweel, J. 2008 On velocity gradients in PIV interrogation. *Exp Fluids* **44**, 831–842.

Westerweel, J., Elsinga, G. E. & Adrian, R. J. 2013 Particle image velocimetry for complex and turbulent flows. *Annu Rev Fluid Mech* **45**, 409–436.